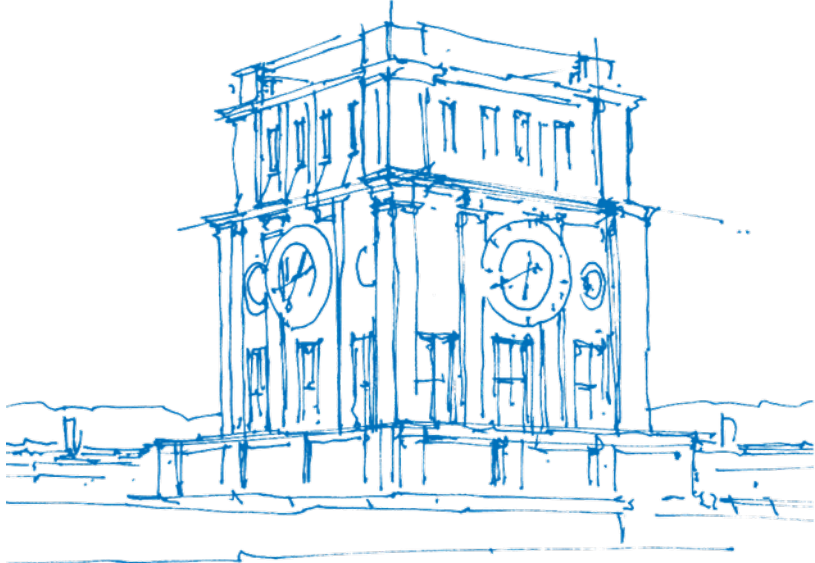


# Local orbit uncertainty reduction in follow-up passes based on single-pass debris laser ranging

Christoph Bamann and Urs Hugentobler

Chair of Satellite Geodesy - Technical University of Munich

9 November 2018



*TUM Uhrenturm*

# Challenges: Orbit determination of space debris with laser tracking

- Many objects, few stations → limited observation times
- **Inaccurate predictions** → no blind tracking possible
- **Terminator** (illumination) and weather (clouds) limitations
- Unfavourable observation geometries
  - ↳ Sparse and ill-distributed tracking data
    - ↳ Observability issues / overfitting
    - ↳ Large estimation uncertainties

# Data fusion with TLE and DISCOS catalog data

- Adds **constraints** for parts of the orbit that cannot be seen by tracking stations in close proximity
- May provide **additional a-priori information** (TLE orbits, mass and cross-section, ...)
- Can use a-priori orbit and uncertainties from **improved TLEs** (SP model fitted to TLE-derived pseudo-observations)
  - ↳ Makes the solution parameters observable in case of unfavorable observation geometries
  - ↳ Avoids overfitting, in particular regarding the ballistic coefficient in LEO
  - ↳ Allows orbit determination even with **single-pass data** in the extreme case

**What is the achievable orbit prediction uncertainty for single-pass debris laser ranging?**

# Force model parameters

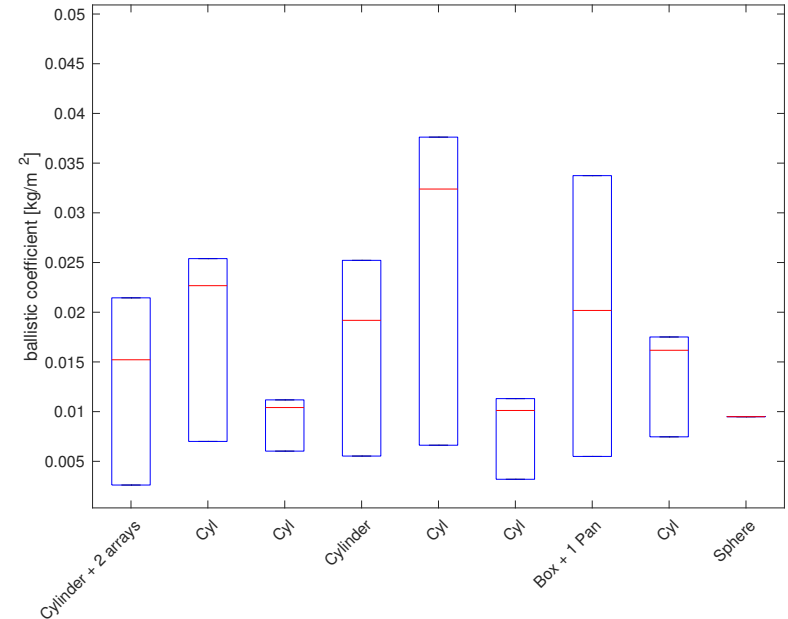
- For very low objects (<500km) good results are obtained if the ballistic coefficient  $BC = C_D \frac{A}{m}$  is estimated using the rate of change of the semi-major axis from historical TLEs:

$$\left. \frac{da}{dt} \right|_{drag} = \frac{2a^2 v}{\mu} \dot{\mathbf{v}}_{drag} \cdot \mathbf{e}_v$$

Together with  $\dot{\mathbf{v}}_{drag} = -\frac{1}{2}\rho BC |\mathbf{v} - \mathbf{V}|^2 \cdot \mathbf{e}_{v-V}$  we obtain:

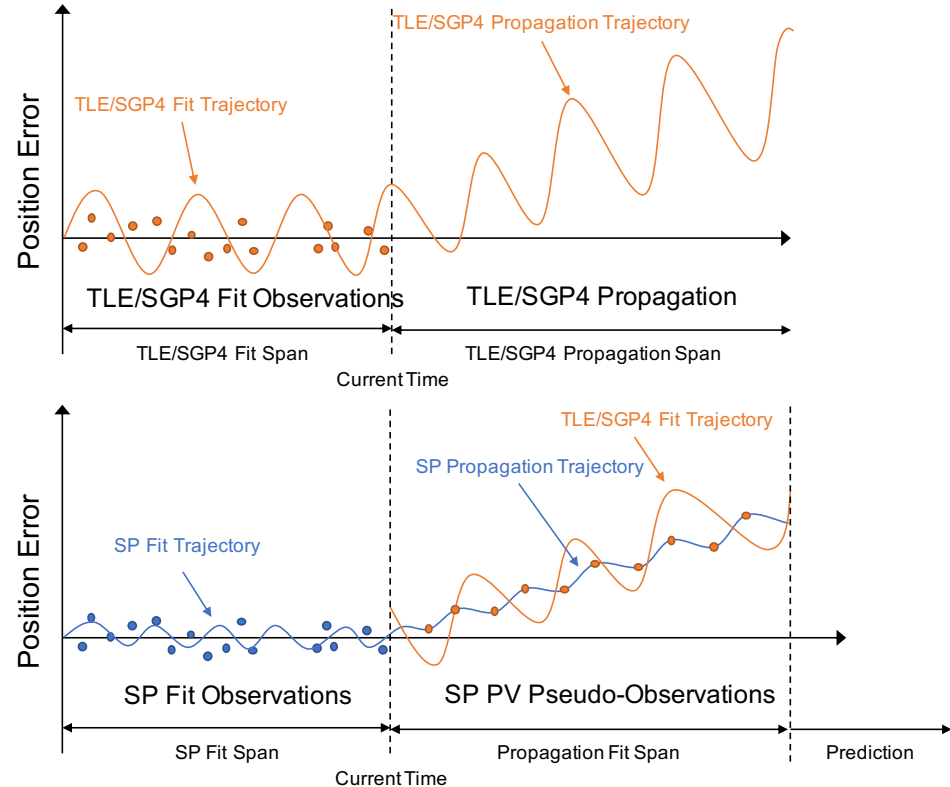
$$BC = -\frac{\mu \Delta a_{t_1, drag}^2}{\sum_{t=t_1}^{t_2} a_t^2 v_t \rho_t \|\mathbf{v}_t - \mathbf{V}_t\|^2 \mathbf{e}_{v_t - V_t} \cdot \mathbf{e}_{v_t} \Delta t}$$

- Object properties (mass, shape, size) from DISCOS - ESA's database and information system characterising objects in space
- The ballistic coefficient and its uncertainty is derived from an object's mass, minimum/average/maximum cross-section and an estimated value for  $C_d$

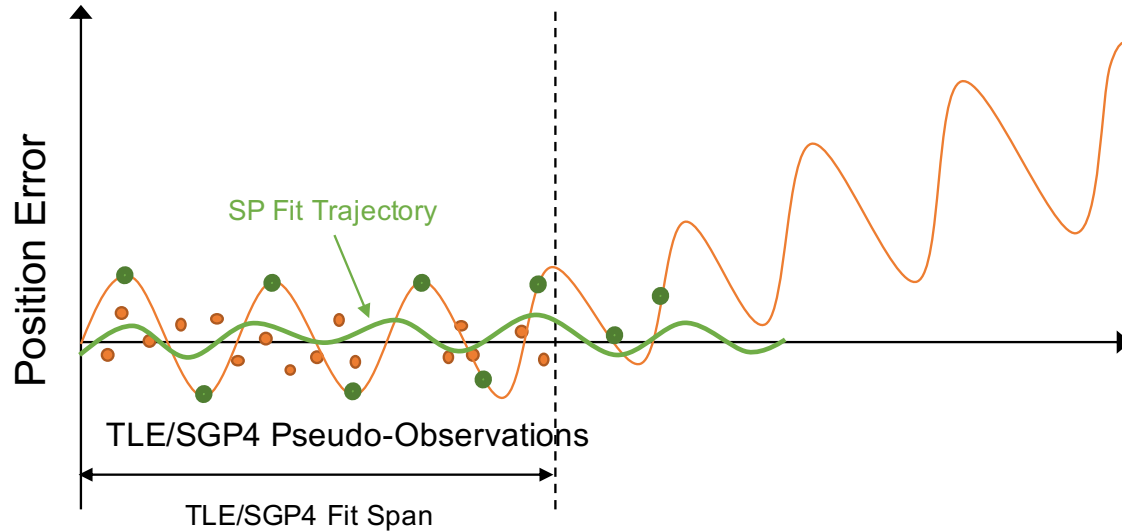


# TLE generation process

- Classical TLEs are generated by fitting an analytical model to real observations
- Since 2013 enhanced TLEs are generated by fitting an analytical model to orbit predictions computed using high-fidelity models

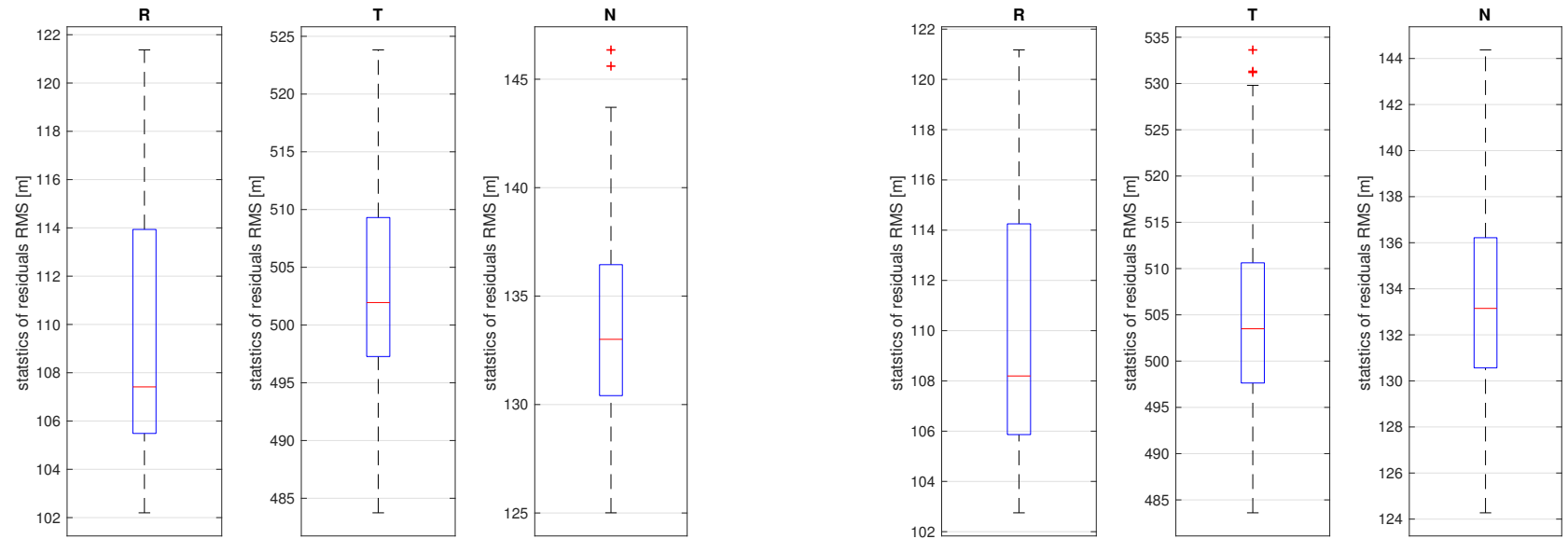


# TLE improvement via SP model fitting



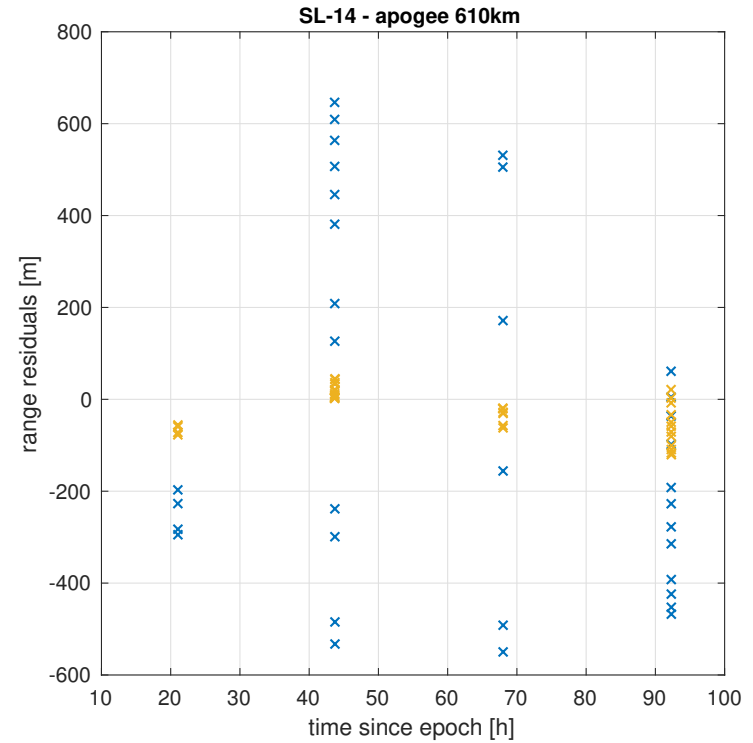
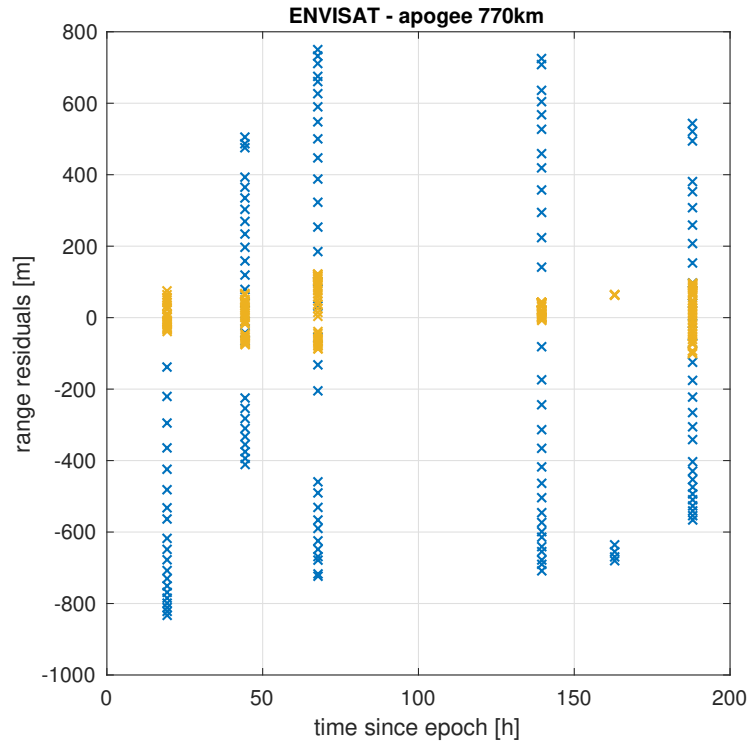
We fit a high-fidelity model to pseudo position-velocity observations from TLEs to obtain a physically more realistic (and improved) orbit

# Statistics of TLE improvement post-fit residuals (RTN frame)



Zenith-2 second stages (left: 22566, right: 22220), altitude  $\approx$  800 km

# Validation using real laser ranging data

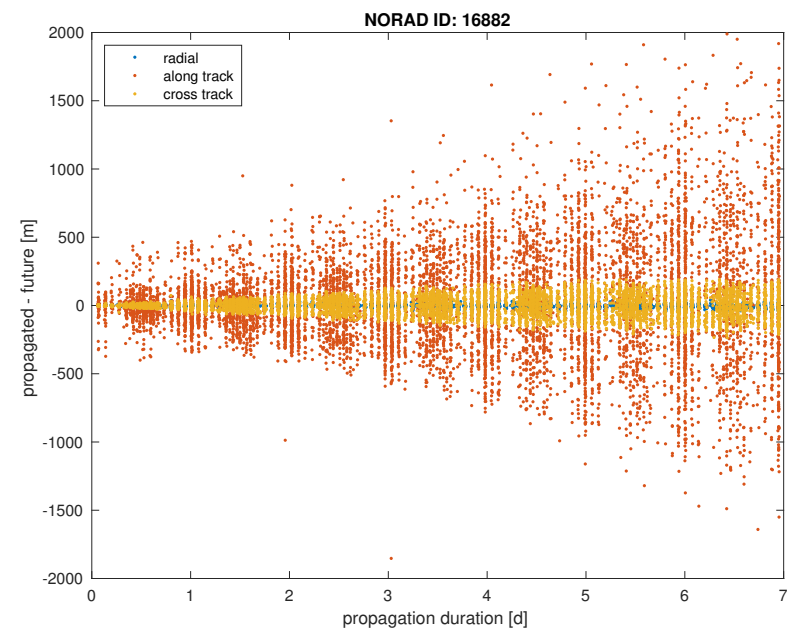
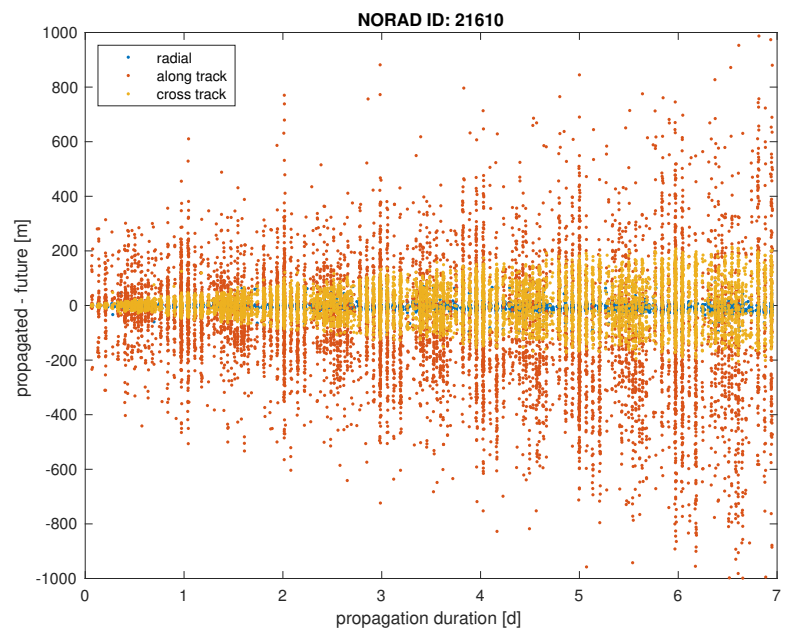




# Uncertainty of improved TLEs

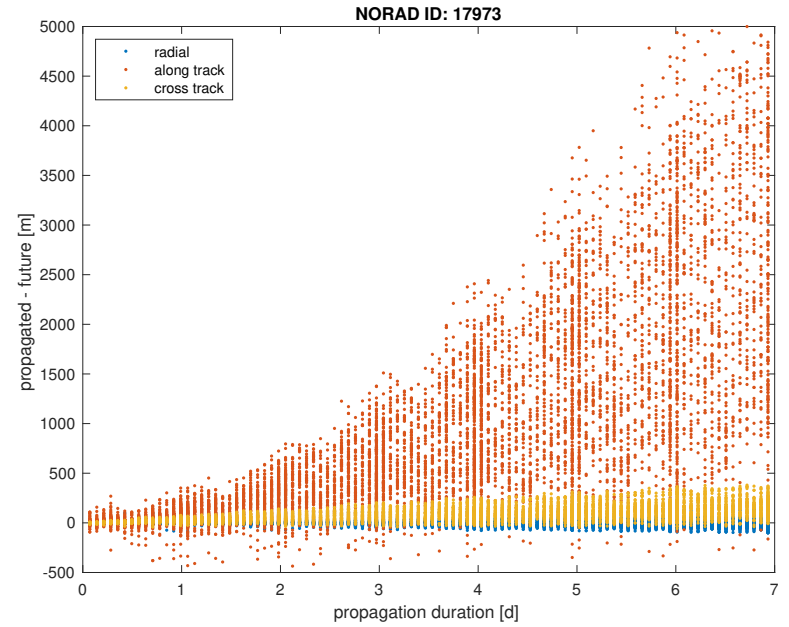
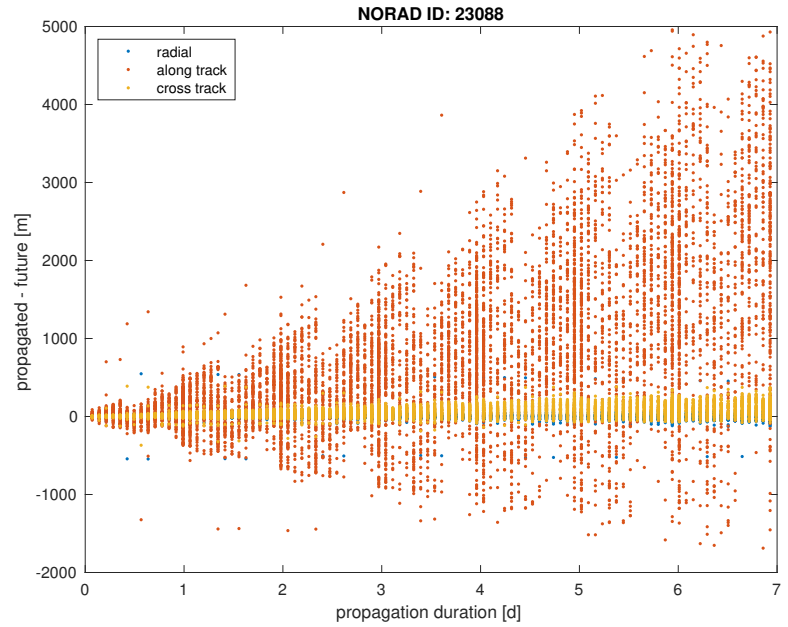
- Several approaches for TLE uncertainty estimation: TLE differencing, RMS after SP-model fitting, ...
  - TLE differencing generally yields non-Gaussian and biased differences that grow polynomially in time
  - OD post-fit residuals using TLEs as pseudo-observations neglect potential TLE biases
- Using an initial state from TLE improvement, we are interested in the uncertainty of this state and not of uncertainty of the underlying TLEs
- We therefore compute differences of TLE improvement solutions from different epochs linked by orbit propagation → these are the samples for covariance estimation

# Differences of improved TLEs at different epochs via propagation (1)



fitted 4 day arc, used BC from historical TLE time series

# Differences of improved TLEs at different epochs via propagation (2)



fitted 4 day arc, used BC from historical TLE time series

# Statistical model of differences of improved TLEs

- In a first-order Taylor series approximation the state-transition matrix  $\Phi(t_2, t_1)$  maps deviations from the reference orbit from one TLE epoch to the next:

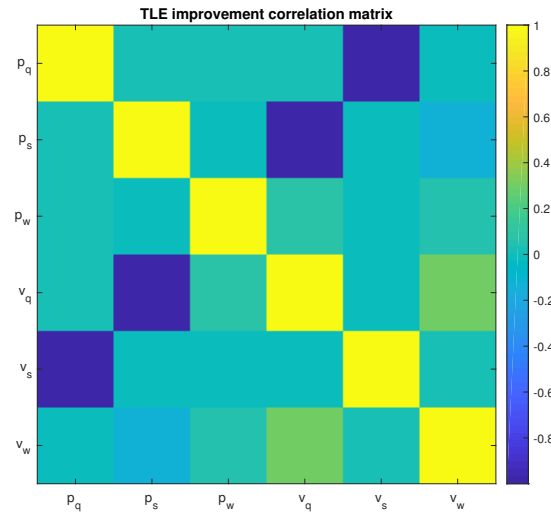
$$\Delta x(t_2) = \Phi(t_2, t_1) \Delta x(t_1)$$

- The **covariance**  $P(t_1)$  is **propagated linearly** via  $P(t_2) = \Phi(t_2, t_1)P(t_1)\Phi(t_2, t_1)^T + Q(t_2, t_1)$ . The additive process noise matrix  $Q(t_2, t_1)$  accounts for integrated force model errors during propagation.
- Consequently, a sample  $d_{j,i} = x(t_j) - \phi(x(t_i); t_j)$  is assumed to be drawn from the following distribution:

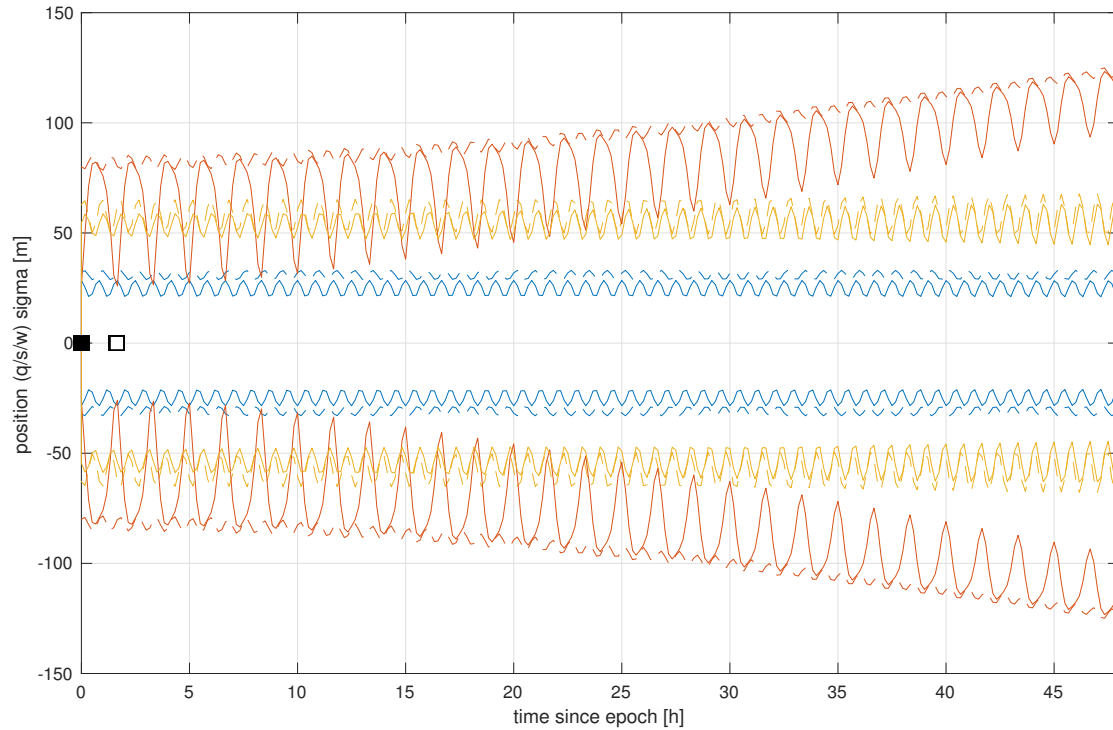
$$d_{j,i} \sim N(0, P(t_j) + \Phi(t_j, t_i)P_i\Phi(t_j, t_i)^T + Q(t_j, t_i))$$

# Correlation matrix of improved TLE

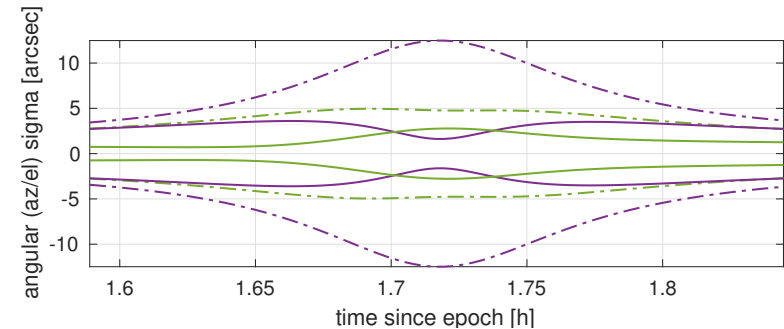
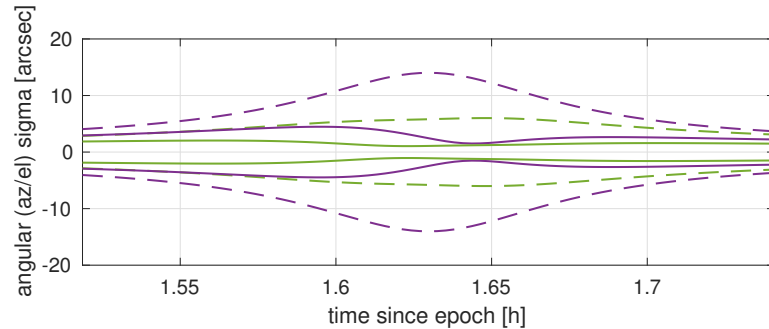
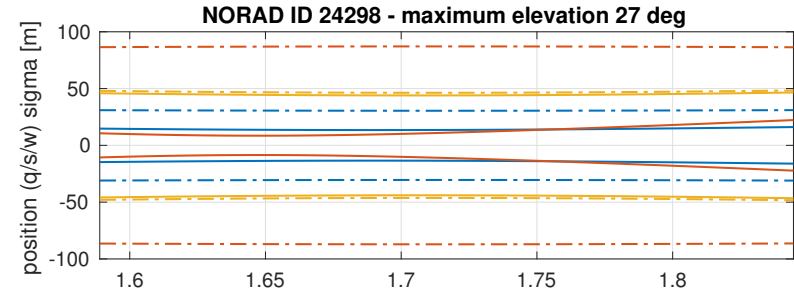
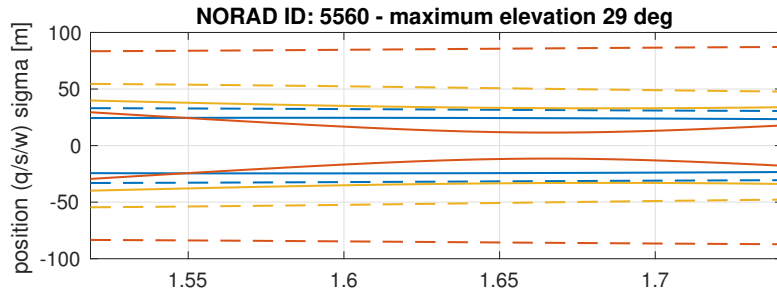
- Assuming  $P(t_j) = P(t_i) = P$  **in the local orbital frame** we maximize the likelihood function  $L = \sum \log f(d_{j,i})$  using an analytical expression for  $Q(t_j, t_i)$ .
- In doing so, we use the **correlation matrix** as obtained from an individual least-squares adjustment for TLE improvement and **estimate only the variances** using the differencing samples.



# Results - Single-pass improvement of RTN uncertainties



# Results - Improved TLE vs. improved TLE + laser



# Results - Covariance ellipsoid vs. pass geometry

- Ranging along the principle direction of covariance ellipsoid...
  - provides maximum information regarding the orbit uncertainty
  - maximizes the likelihood of hitting the target in bind tracking
- Potential approaches to quantify this:
  - 1D: Based on projection of normalized view direction vector  $\frac{\mathbf{v}_{view}}{\|\mathbf{v}_{view}\|}$  onto principal axis vector  $\mathbf{u}_1$  of the covariance ellipsoid  $P_{pos}$

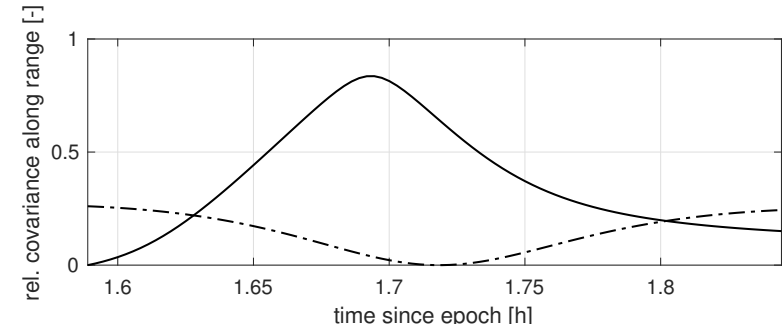
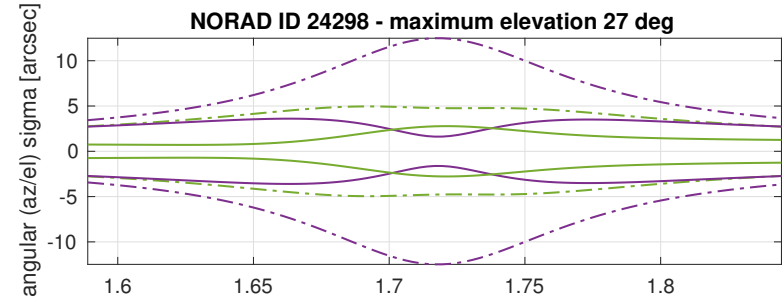
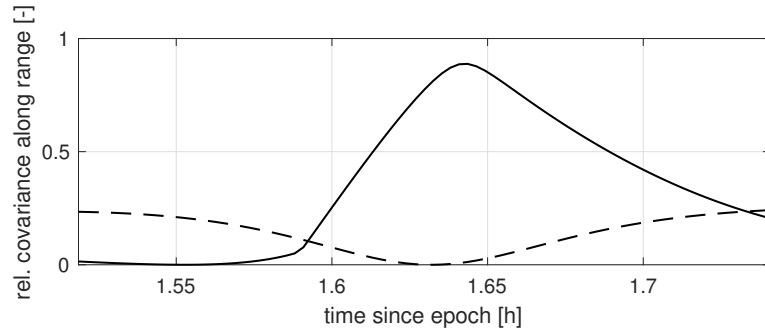
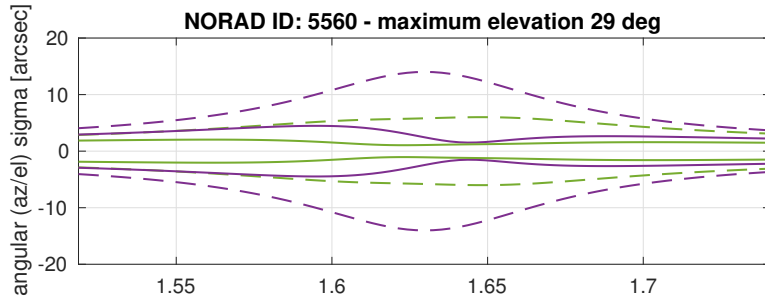
$$\left\langle \frac{\mathbf{v}_{view}}{\|\mathbf{v}_{view}\|}, \mathbf{u}_1 \right\rangle \quad (1)$$

- 2D: Using area  $A_{view}$  of covariance ellipse projected onto view direction and area  $A_{12}$  of covariance ellipse along the two principal axes

$$1 - \frac{A_{view}}{A_{12}} \quad (2)$$



# Results - Improved TLE vs. improved TLE + laser



## Results - Quality testing via filter consistency

- Under the hypothesis that the filter is consistent, the **normalized innovation squared** at  $t = t_k$

$$\varepsilon_v(k) = v(k)^T S(k)^{-1} v(k) = v(k)^T (H(k)P(k|k-1)H(k)^T + R)^{-1} v(k) \quad (3)$$

has a **chi-squared distribution** with  $n_z$  degrees of freedom, where  $n_z$  is the dimension of the measurement, i.e. equal to one for range measurements.

- From  $N$  **independent samples**  $\varepsilon_v(k)^i$  one calculates the average

$$\bar{\varepsilon}_v(k) = \frac{1}{N} \sum_{i=1}^N \varepsilon_v(k)^i \quad (4)$$

which is then tested with acceptance region determined based on the fact that  $N\bar{\varepsilon}_v(k)$  is chi-square distributed with  $Nn_z$  degrees of freedom.

# Results - Comparisons and filter consistency

|   | max. cov. range [% of pass] | sig_max az/el [arcsec] | rel. estimation consistency | rel. prediction consistency |
|---|-----------------------------|------------------------|-----------------------------|-----------------------------|
| <b><u>22566 (maximum elevation first / follow up pass: 22° / 53°)</u></b> |                             |                        |                             |                             |
| Impr. TLE   | 1                           | 29 / 10                | –                           | 1.00                        |
| Impr. TLE + laser   | 48                          | 17 / 9                 | 0.92                        | 0.95                        |
| <b><u>23088 (maximum elevation first / follow up pass: 30° / 58°)</u></b> |                             |                        |                             |                             |
| Impr. TLE   | 3                           | 34 / 12                | –                           | 1.00                        |
| Impr. TLE + laser   | 42                          | 7 / 4                  | 1.00                        | 1.00                        |
| <b><u>24298 (maximum elevation first / follow up pass: 44° / 27°)</u></b> |                             |                        |                             |                             |
| Impr. TLE   | 1                           | 12 / 5                 | –                           | 0.73                        |
| Impr. TLE + laser   | 42                          | 4 / 3                  | 1.00                        | 1.00                        |
| <b><u>27386 (maximum elevation first / follow up pass: 24° / 26°)</u></b> |                             |                        |                             |                             |
| Impr. TLE   | 1                           | 13 / 6                 | –                           | 1.00                        |
| Impr. TLE + laser   | 56                          | 6 / 5                  | 1.00                        | 0.80                        |
| <b><u>5560 (maximum elevation first / follow up pass: 27° / 29°)</u></b>  |                             |                        |                             |                             |
| Impr. TLE   | 100                         | 14 / 6                 | –                           | 0.92                        |
| Impr. TLE + laser   | 57                          | 4 / 2                  | 0.88                        | 1.00                        |

# Summary

- Extended Kalman Filter framework for data fusion of laser ranges with TLEs
- Force model parameters from historical TLEs and the DISCOS database
- Developed an uncertainty estimation method for improved TLEs
- Tested improved TLEs & TLE-laser data fusion based on real data
- Significant reduction of uncertainty for telescope pointing in follow-up passes
- Highest chance of "hitting" target shifts from edges to middle of a pass

# Outlook

- Use predicted uncertainties to derive search strategies for blind tracking
- Blind tracking campaign?